Brazilian Journal
of Chemical
Engineering

ISSN 0104-6632
Printed in Brazil
www.abeq.org.br/bjche

Vol. 36, No. 01, pp. 229 - 237, January - March, 2019
dx.doi.org/10.1590/0104-6632.20190361s20180030

RHEOLOGICAL BEHAVIOR OF A SILVER AQUEOUS NANOFLUID STABILIZED WITH AMINOSILANE-BASED SURFACTANT UNDER CONFINED FLOW

Júlia C. Kessler[1], Natan Padoin[1], Dachamir Hotza[1] and Cíntia Soares[1*]

[1] Universidade Federal de Santa Catarina, Departamento de Engenharia Química e de Alimentos, Florianópolis, SC, Brasil.
E-mail: cintia.soares@ufsc.br, ORCID: 0000-0001-9273-2329; ORCID: 0000-0002-7247-2934;
ORCID: 0000-0002-7086-3085; ORCID: 0000-0002-4411-8305

(Submitted: January 22, 2018 ; Revised: July 25, 2018 ; Accepted: August 31, 2018)

Abstract - The rheological behavior of an aqueous suspension of silver nanoparticles stabilized with aminosilane-based surfactant flowing under confinement was investigated. Three stability levels were defined based on the zeta potential: high (41.73 mV, pH 4.3), medium (10.44 mV, pH 7.4), and low (0.74 mV, pH 8.6). Furthermore, the preliminary investigation showed that the surface charge remained positive, and the formation of agglomerates was not observed. Due to the particle coating and the ionization of the amino groups of the surfactant an electrosteric stabilization was evidenced. Shear rates ranging from 50 to 1000 s^{-1} and shear stresses between 0.02 and 0.2 Pa, at the temperatures of 15, 25 and 35 ºC, were evaluated with the nanofluid flowing in microchannels with a gap of 100, 300 and 500 μm. A trend to dilatant behavior was observed at high shear rate and a slit size of 500 μm, while Newtonian behavior was predominant at lower slit sizes. A reduction of 47.3% was noticed at 25 ºC with the variation in the slit size from 500 to 300 μm. Furthermore, the viscosity of the nanofluid decreased as much as 60% when the slit size was reduced from 500 to 100 μm.
Keywords: Nanofluid; Silver; Functionalization; Rheology; Microfluidics.

INTRODUCTION

A suspension of nanoparticles, with size ranging from 1 to 100 nm in at least one dimension (Delay et al., 2011), is known as a nanofluid. These nanosuspensions can exhibit singular properties depending on the particle size distribution and shape, concentration, density, as well as pH and presence of additives. Several methods for preparation, dispersion and optimization of nanofluids have been described in the literature (Kumpulainen et al., 2011; Shi et al., 2011; Mahbubul et al., 2012; Keramati et al., 2015; Du et al., 2016).

Additives have been frequently used in the preparation of nanofluids for the functionalization of the surface of the nanoparticles, promoting stability (Ghamidi et al., 2011) and avoiding agglomeration through the action of steric and electrostatic repulsive forces (Lin et al., 2012).

Recently, there is an increased interest in the investigation of the flow of nanofluids in confined structures. Application of nanofluids in microchannels can be found in microelectronics, energy generation, biomedicine, and manufacture of nanostructures. In all cases, however, the rheological behavior of the nanosuspension in microfluidic devices has been reported as complex (Sundar and Sharma, 2010; Sridhara and Satapathy, 2011; Mohammed et al., 2011; Hojjat et al., 2011; Haghighi et al., 2015).

Sharma et al. (2016) considered the particle nature, concentration, base fluid, stabilization method, shear rate and shear stress for a phenomenological

* Corresponding author: Cíntia Soares - E-mail: cintia.soares@ufsc.br

evaluation of several nanofluids. Moreover, Sohrabi et al. (2016) modeled nanofluid flow in a microfluidic device considering the particle interaction, geometry of the microchannel, shear rate, density and particle size distribution.

According to Hojjat et al. (2011), the rheological behavior of nanofluids can change from Newtonian to non-Newtonian depending on the concentration of nanoparticles. Furthermore, viscosity reduction was also reported when increasing the shear rate (Tamjid and Guenther, 2010). Clogging and particle aggregation (Georgieva et al., 2010; Chandrasekar et al, 2010) and stability of the flow regime (Ho et al., 2010; Singh et al., 2012) were also reported when flowing nanofluids through microchannels. However, Chen et al. (2007) reported that hydrodynamic forces can be insufficient to break up the aggregates of particles into individual primary particles.

Based on this scenario, the importance is evident of comprehensive investigation of the rheology of nanofluids flowing in microchannels, given the complexity associated with this phenomenon and the increased search for applications of these systems. This work focuses on the investigation of the rheology of a nanofluid consisting of silver nanoparticles dispersed in water and stabilized with an aminosilane-based surfactant flowing under confinement. Silver nanoparticles have been used as antimicrobial agents, for instance. When in aqueous suspensions, additives such as surfactants are used to ensure stability (*i.e.*, absence of agglomeration). Giving that this functionalized nanofluid can flow through confined spaces in several instances, it is of paramount importance to know its rheological properties for proper design and optimization of the equipment. That is, precisely, the novelty of this work.

MATERIAL AND METHODS

A commercially available nanofluid was kindly provided by *TNS Nanotechnology* (Florianópolis/SC, Brazil). This nanosuspension consists of silver nanoparticles, synthesized by reduction of silver nitrate ($AgNO_3$), dispersed in water and stabilized with an aminosilane-based surfactant. A preliminary characterization revealed morphological and physical-chemistry properties of the nanofluid, used as commercialized without any additional treatment. Then, the rheological performance in confined space was evaluated.

The particle size distribution was determined in a dispersion analyzer (LUMiSizer, 6110- 87, Germany). The equipment was operated at 25 ºC, with a light factor of 1.0. The same principle adopted for the evaluation of static sedimentation was applied herein, using centrifugal force for shortening total analysis time and infrared light transmission to determine the particle size profile along time. The tests were carried out in duplicate.

Mass concentration of the nanoparticles in the suspension was determined by flame atomic absorption spectroscopy (FAA, Perkin Elmer, PINAACLE 900T, USA) and the mean free path of the particles (λ) was calculated from Fullman's equation (1953) as $\lambda = (2/3)\, d_p(1-\phi_p)/\phi_p$, where d_p is the average particle size and ϕ_p is the volumetric fraction of the particles. Pycnometry was used to determine the density of the nanofluid.

Transmission electron microscopy (TEM, Jeol JEM-1011 Electron Microscope, Japan) images were obtained with a maximum voltage of 100 kV, on all samples.

Measurements of zeta potential (Stabino, Particle Metrix, Germany) were performed with automatic titration of sodium hydroxide (0.01 N) over the pH range of 3.0 to 10.0. Based on the results obtained from this technique, three stability levels (high, medium and low) were defined within the pH range and further experiments were performed at the chosen pH values.

The rheological behavior of the stabilized silver nanofluid was analyzed through rotational rheometry (Haake, Mars II, Germany), using parallel plates with 35 mm diameter and adjustable size. Shear rates ranged from 50 to 1000 s^{-1}, with shear stress between 0.02 and 0.2 Pa. The rheometer operated in controlled stress (CS) mode that enabled normal force measurements within the range of 0.01 N to 50 N with uncertainty in viscosity measurements of ± 5% for the slit size of 500 μm, according to the equipment manufacturer (FISCHER, 2007).

Measurements were carried out at three different temperatures (15, 25 and 35 ºC), keeping all other conditions constant. Additionally, the experimental data were compared with the Newtonian ($\tau = \mu_f \,.\, \gamma$, where τ is the shear stress, μ_f is the viscosity of the nanofluid and γ is the shear rate), Power Law ($\tau = \mu_f \,.\, \gamma_\eta$, where $\eta < 1$ and $\eta > 1$ imply in pseudoplastic and dilatant fluids, respectively) and Herschel-Bulkley ($\tau = \tau_0 + \mu_f \,.\, \gamma^\eta$, where τ_0 corresponds to the initial shear stress) models.

A non-fractional factorial design with three factors evaluated at three levels was applied, resulting in 27 experiments (see Table 1), aiming to determine the effect of these parameters on the nanofluid viscosity when reaching a shear rate of 1000 s^{-1}.

Table 1. Factorial design for the characterization of the nanofluid.

Stability Level	pH value	Slit size (μm)	Temperature (ºC)
High	4.3	100	15
Medium	7.4	300	25
Low	8.6	500	35

The Reynolds number was calculated [$Re = (\rho . \Omega . L^2)/\mu_f$] and the possible occurrence of a secondary flow was analyzed (Ewoldt et al., 2015).

The data were interpreted using a statistical software (Statistica 10, Statsoft) at a confidence interval of 95% for the variance analysis (ANOVA) through Tukey's test.

RESULTS AND DISCUSSION

Preliminary characterization of the nanofluid

The average size of the silver nanoparticles was 30 nm, with D_{50} of 21 nm. A multimodal distribution was observed, with minimum size of 13 nm (<10% of the suspended content). Tamjid and Guenther (2010) and Aberoumand et al. (2016) reported silver nanofluids with particles sizes of 40 and 20 nm, respectively, which is in accordance with the results obtained herein. Moreover, the particle size measurements were corroborated by the TEM images, as reported in Fig. 1. Similar characteristics were also described by Paul et al. (2012) and Mahbubul et al. (2012).

The density of the nanofluid measured at 25 ºC was 0.9612 g·mL^{-1}. Moreover, the concentration of the silver nanoparticles, determined by FAA, was 956 mg·L^{-1} (~0.096 wt.% or ~0.087 vol.%). Although results for aqueous silver nanosuspensions stabilized with aminosilane-based surfactant are not available in the literature for direct comparison with the data reported herein, the characteristics of other nanofluids can be used as a reference. Rao et al. (2015) obtained different values for the density of alumina nanosuspensions in water as a function of the concentration: 1.1015 g·mL^{-1} at 0.035 vol.%, 1.0714 g·mL^{-1} at 0.025 vol.%, and 1.0416 g·mL^{-1} at 0.015 vol.% solids. Shoghl et al. (2016), on the other hand, determined the density of different nanofluids as a function temperature, with different surfactant concentrations. The density of the base fluid (water + surfactant) was 0.996 g·mL^{-1} for 0.02 wt.% sodium dodecylsulfate (SDS) at 30 ºC, while at 40 °C the value of this parameter decreased to 0.992 g·mL^{-1}.

The mean free path estimated by Fullman's equation was 16 nm. According to Chen et al. (2007), this is a semiconcentrated nanofluid (~0.05 to 0.1) vol.%, with possible non-Newtonian behavior. Higher concentrations of the nanoparticle could not be reached due to hindered dispersion of particles, possibly due to limitation of the dispersing capacity of the surfactant. It should be highlighted, though, that higher concentrations (0.12 to 0.72 wt.%) of silver nanoparticles were reported when dispersed in oil (Aberoumand et al., 2016). Moreover, Parametthanuwat et al. (2015) worked with an aqueous suspension of silver nanoparticles with sizes varying from 95 to 100 nm (non-stabilized with surfactant as in this work) with concentration of 0.5 wt.%. Additionally, Singh and Raykar (2008), Chen et al. (2010), Oliveira et al. (2014) and Afrand et al. (2016) reported silver nanosuspensions with concentrations of (1.0, 16.0, 0.3 and 1.2) vol.%, respectively.

The zeta potential of the nanoparticles in suspension was measured as a function of pH and the result is reported in Fig. 2. Values of the zeta potential associated with stable suspensions (>30 mV) are clearly observed for pH around 4, reaching ~42 mV at pH 4.3, which corresponds to a positively charged surface. The stability of the silver nanoparticles in water is then steadily reduced for higher values of pH and the isoelectric point is reached in the pH range of 8.6-10. Therefore, three stability levels were defined for the rheological investigations at the pH corresponding to the highest, intermediate and lowest values of zeta potential (*i.e.*, highest, intermediate and lowest levels of stability). It should be highlighted that

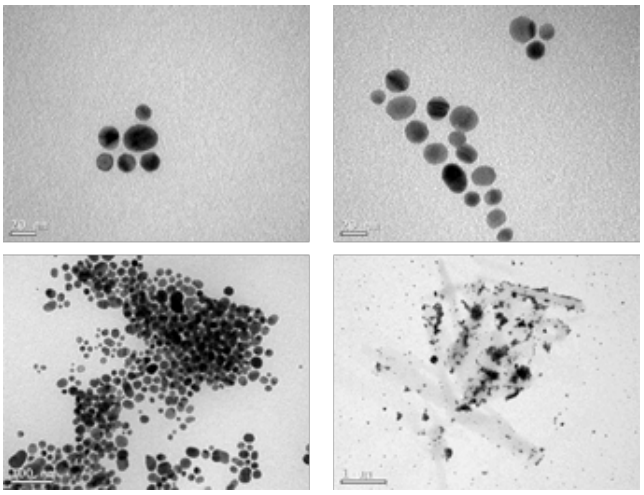

Figure 1. TEM images evidencing the morphology and the particle size of silver nanoparticles in an aqueous suspension, stabilized with aminosilane-based surfactant, at different magnifications.

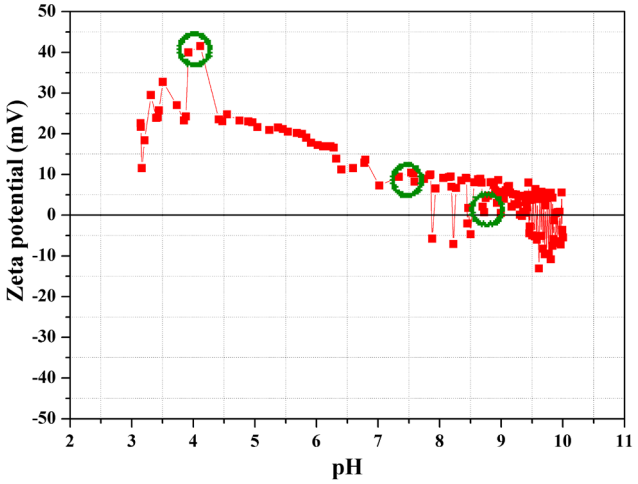

Figure 2. Stability levels of the nanofluid according to the zeta potential as a function of pH.

the nanofluid is commercialized with a pH of 3.1 (zeta potential of 22.60 mV).

Different results were obtained by Sadowski et al. (2008), Elzey and Grassian (2010), and Leo et al. (2013) for silver nanoparticles in suspension. In all cases, the charge at the surface was negative and the isoelectric point was located at the acid pH of 2.0, 2.5 and 3.0, respectively. Therefore, both the nature of the charges and the values of the isoelectric point are not in agreement with the results obtained in this work. It should be highlighted, though, that in these cases the silver nanoparticles received different treatments compared to the one applied in this work. Thus, the differences observed might be attributed to the stabilization of the aqueous silver nanoparticles with the aminosilane-based surfactant.

The behavior of aqueous silver nanosuspension treated with aminosilane-based surfactant can be explained with the scheme presented in Fig. 3.

According to Parks (1965), the isoelectric point of the silver nanoparticles (without treatment) corresponds to pH in the range 1.5 – 3.5. Aggregation can occur when the pH is changed to values out of this interval or due to the addition of electrolytes to the solution. However, when a surface treatment is applied, using aminosilane-based surfactant for instance, the nanoparticles can remain stable even in a pH range different from that corresponding to the isoelectric point of untreated silver, due to the formation of a steric layer with ionizable groups (Loftizadeh et al., 2016).

The aminosilane-based surfactant can ionize completely and shift the zeta potential to the acid pH range. Silver nanoparticles, which have naturally negative surface charges, are fully coated as the surfactant ionizes, reacting with hydroxyl groups at the particle surface. Thus, there is a saturation of positive charges at low pH. Therefore, the silver nanoparticles do not agglomerate due to the repulsive electrostatic forces. As the pH is increased to neutral or alkali ranges, though, this behavior is not observed, and the zeta potential is close to zero. Under this condition, van der Waals forces become significant and the particles tend to agglomerate.

A simplified ionization mechanism of the amino groups in contact with the surface of silver nanoparticles, in acid medium, is suggested as

$$Ag^{-}_{(s)} + AM^{+}_{(l)} + H_2O_{(l)} + HX \rightarrow Ag^{*}_{(s)} + H_3O^{+}_{(l)} + X^{-} \qquad (1)$$

where $Ag_{(s)}^{-}$ represents the silver nanoparticle, $AM_{(l)}^{+}$ is the aminosilane surfactant, $H_2O_{(l)}$ is the reaction medium, HX is an acid, $Ag_{(s)}^{*}$ represents the silver nanoparticle with surface modification, $H_3O_{(l)}^{+}$ is the hydronium ion formed and X^{-} is an anion.

Rheological behavior of the nanofluid under confined flow

The evaluation of the rheological behavior of the nanofluid under confinement (microchannels) was performed in a parallel plate rotational rheometer, as described in section 2. The same procedure was used by Hedayati and Domairry (2015) for the rheological evaluation of titanium dioxide nanofluid under confinement.

Figures 4, 5 and 6 present, respectively, the rheological behavior of the silver nanofluid stabilized

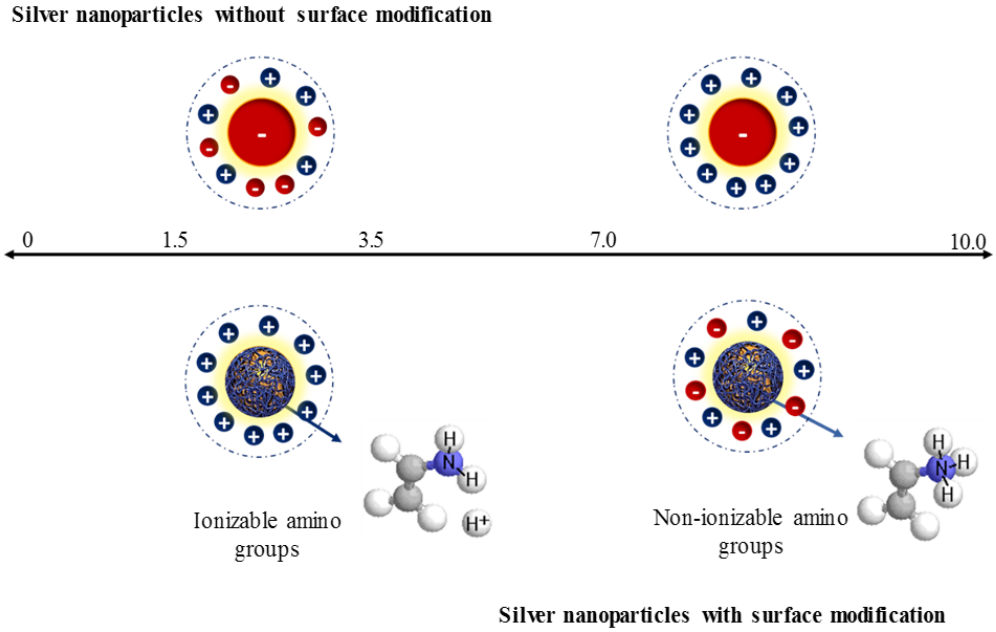

Figure 3. Scheme representing the action of aminosilane-based surfactant on silver nanoparticles in an aqueous medium at different pH values.

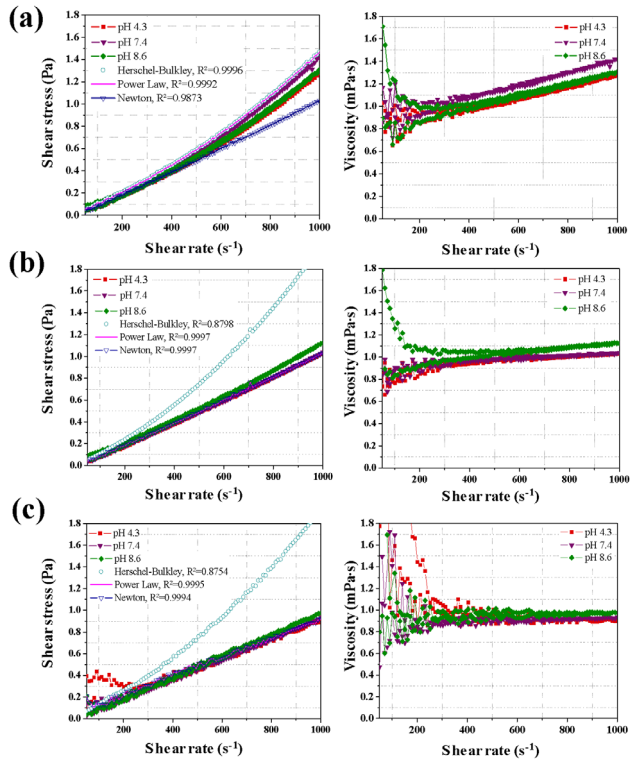

Figure 4. Shear stress and viscosity as a function of shear rate for the nanofluid at 15 ºC, considering three stability levels (pH) and slit sizes of (a) 500 µm, (b) 300 µm and (c) 100 µm.

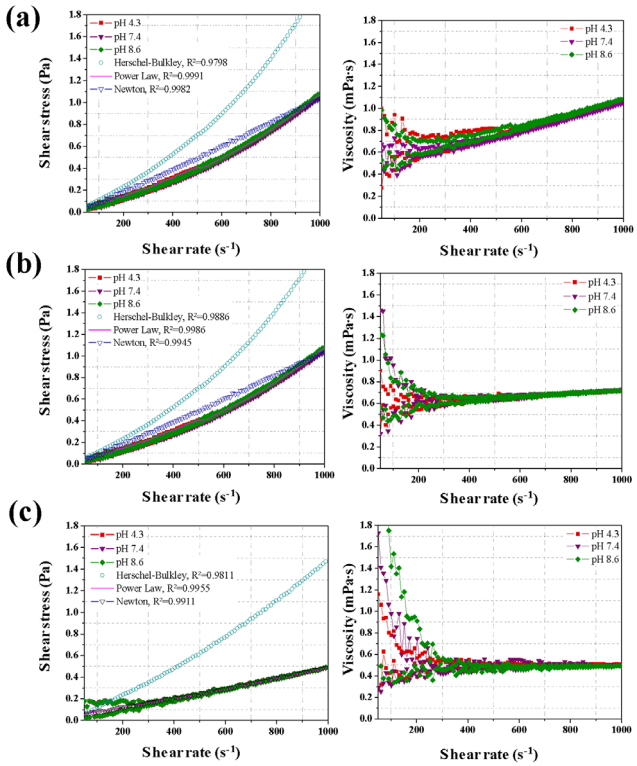

Figure 5. Shear stress and viscosity as a function of shear rate for the nanofluid at 25 ºC, considering three stability levels (pH) and slit sizes of (a) 500 µm, (b) 300 µm and (c) 100 µm.

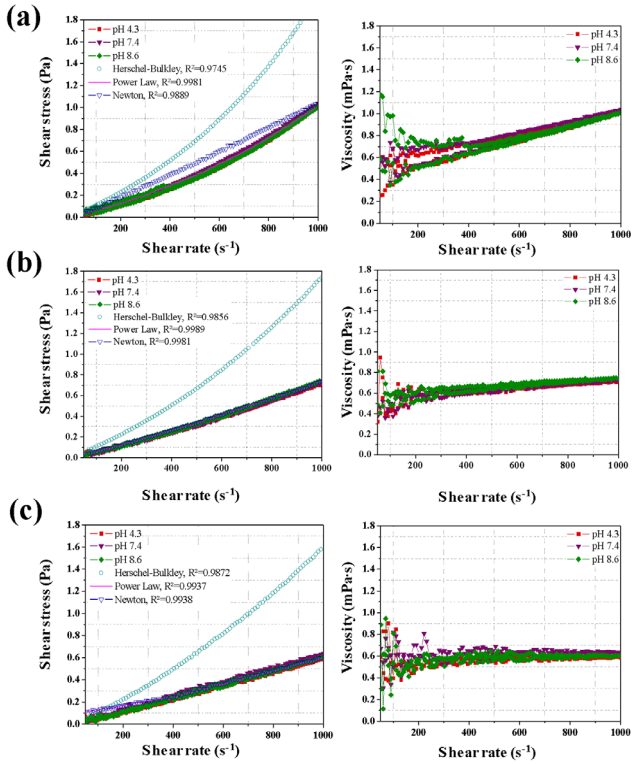

Figure 6. Shear stress and viscosity as a function of shear rate for the nanofluid at 35 ºC, considering three stability levels (pH) and slit sizes of (a) 500 µm, (b) 300 µm and (c) 100 µm.

with aminosilane-based surfactant at 15 ºC, 25 ºC and 35 ºC for three pH values (corresponding to the lowest, intermediate and highest level of stability as previously defined) and three slit sizes: (a) 500 µm, (b) 300 µm and (c) 100 µm.

A tendency of dilatant behavior was observed for high shear rates at the larger slit size (500 µm). As the slit size was reduced, though, the nanofluid exhibited Newtonian behavior. This trend was observed for all temperatures evaluated. Moreover, the power-law model presented the best fit for all cases ($R^2 \approx 1$).

Rheological behavior of the silver nanofluid was not related to that of the aminosilane-based surfactant, as can be confirmed by Fig. 7. Rheological results indicated that the behavior of the surfactant

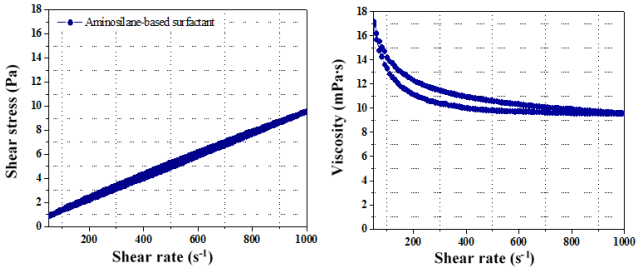

Figure 7. Shear stress and viscosity as a function of shear rate for the aminosilane-based surfactant at 25 ºC and slit size of 500 µm.

was Newtonian with a correlation of 0.9940. The analysis was conducted at 25 ºC and slit size of 500 µm. The surfactant showed a small hysteresis and suggests thixotropic behavior. In this condition, the aminosilane-based surfactant presented a viscosity 13 times bigger than the nanofluid.

Non-linearity was also observed by Mostafizur et al. (2014) when working with alumina and titanium dioxide nanofluids. The dilatant behavior was predominant for temperatures ranging from 1 to 20 ºC, with concentrations in the range of 0.01 – 0.15 vol.%.

No evident differences were noted for the different pH values (stability levels), maintaining all other conditions constant. Furthermore, no time variation of the profiles of viscosity and shear stress was noticed. In addition, no hysteresis was found in these profiles.

The viscosity decreased as the slit size was decreased, reaching a reduction of 47.3% when the size changed from 500 to 300 µm at 25 ºC. Viscosities in the range of (0.585 – 0.974) mPa·s, (0.716 – 1.124) mPa·s and (1.008 – 1.417) mPa·s were measured as a function of the slit sizes of 100, 300 and 500 µm, respectively. Moreover, the influence of temperature on the rheology of the nanofluid can be observed in the values of viscosity measured at the shear rate of 1000 s^{-1}. Keeping the slit size constant, there was a decrease in the viscosity of ~25.2% when the temperature varied from 15 to 25 ºC, while a variation of ~4.6% was observed from 25 to 35 ºC. Fig. 8 shows the values of viscosity obtained at different temperatures and slit sizes for the shear rate in the range of 800 - 1000 s^{-1}.

The viscosity decreased as the temperature increased, which agrees with the works of Namburu et al., (2007), Kole and Dey (2010) and Hojjat et al. (2011) when working with different nanofluids. Interestingly, at the temperature of 35 ºC the average valued of viscosity measured was slightly higher than at 25 ºC for the slit sizes of 300 and 100 µm, even though the error associated with these measurements does not allow one to precisely define a tendency. Chen et al. (2008) observed a similar effect at temperatures above 55 ºC when working with carbon nanotubes suspended in distilled water, ethylene glycol and glycerol.

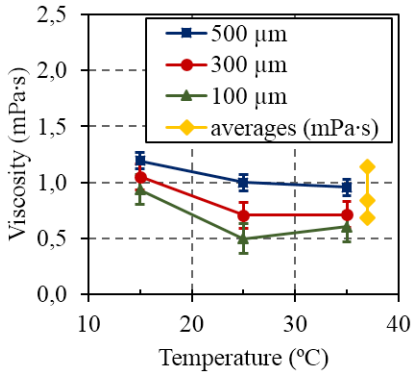

Figure 8. Viscosity at the shear rate in the range of 800-1000 s^{-1} as a function of temperature and slit size. Average viscosities for the slit sizes of 100, 300 and 500 µm are also shown.

Therefore, it is evident that the behavior of nanofluids flowing at the microscale is distinct from that observed at the macroscale. Smaller dimensions provided a viscosity reduction higher than 60%, which represents a significant advantage in terms of microfluidic applications. This data can be observed in Fig. 8 (yellow line) with average viscosities of ~1.14, ~0.84 and ~0.68 mPa·s for the slit sizes of 500, 300 and 100 µm, respectively. However, it should be considered that the efficiency of microflow of nanofluids is dependent on the functionalization of the nanoparticles.

Yao and Kim (2002) obtained a different behavior when using polymeric materials. An increase of up to 130% in viscosity was reached when the polymer flows through a slit of 0.1 µm when compared with a condition of non-confinement.

Moreover, although there was a tendency of dilatant behavior, corresponding to a viscosity increase at high shear rates, this phenomenon was not due to an agglomeration process, as mentioned by Mahbubul et al. (2013) and Mostafizur et al. (2014), since the original value of viscosity was reached as the shear rate decreased (*i.e.*, absence of hysteresis).

Using the average viscosity (as a function of temperature and pH) at each slit size, the Reynolds number and the steady shear viscosity were calculated: 0.1004, 0.0294 and 0.0013 for the slit sizes of 500, 300 and 100 µm, respectively. Therefore, Re_{crit} (=12.0, considering an error of ~3% for pure water at 25 ºC and slit size of 500 µm) was not reached in any experiment. Thus, the experimental limit of steady shear viscosity [$\mu_f(\gamma)$] was not exceeded and the results obtained do not correspond to a possible secondary flow (data not shown) (Ewoldt et al., 2015).

The response surface graphs presented in Fig. 9 summarize the combined influence of slit size × pH, temperature × pH and temperature × slit size. Clearly, the slit size and temperature have significant influence on the viscosity of the nanofluids at high shear rates.

Finally, the statistical analysis revealed a relevant effect of the slit size and the temperature, at high shear rates, on the viscosity of the nanofluid. Table 2 shows the ANOVA, where the non-significance of the pH is evidenced. However, all combinations of factors influenced the dependent variable. The values of *p* close to zero indicate that the data were not random, with a confidence level of 95%.

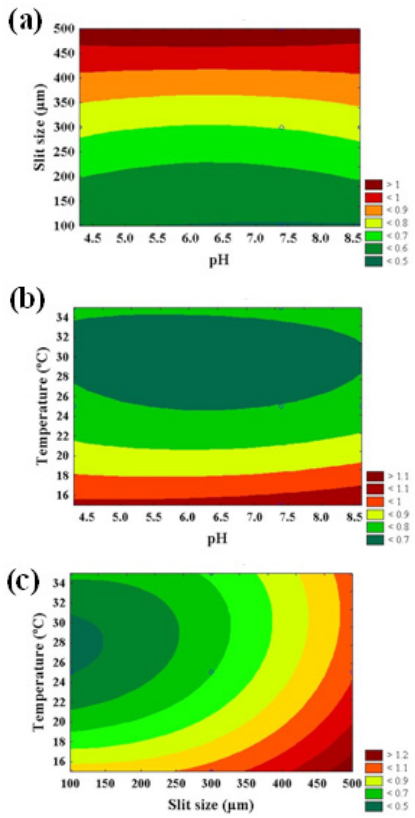

Figure 9. Response surface graphs for the viscosity (mPa·s) as a function of (a) the slit size and pH, (b) temperature and pH, and (c) temperature and slit size.

Table 2. Variance analysis (ANOVA) for the evaluation of factors capable of influencing the nanofluid viscosity, measured at the shear rate of 1000 s^{-1}.

Factor	Factor F	p
pH	0.0	0.28
Slit size (µm)	385.9	0.00
Temperature (ºC)	269.5	0.00
pH × slit size (µm)	0.6	0.63
pH × temperature (ºC)	0.9	0.50
Slit size × temperature (ºC)	5.9	0.02

* $p < 0.05$; $p \approx 0 \rightarrow$ non-random results.

CONCLUSIONS

A nanofluid consisting of an aqueous suspension of silver nanoparticles stabilized by aminosilane-based surfactant was characterized in terms of morphological and physical-chemistry properties. Then, the rheological behavior of the nanosuspension was evaluated considering three levels of stability (regarding the zeta potential), three values of temperature (15, 25 and 35 ºC) and three slit sizes for a rotational rheometer (100, 300 and 500 µm), in order to simulate conditions of confined flow.

The rheological behavior of the silver nanofluid was dependent on the different sizes of the microchannels evaluated. At 500 µm, a tendency to dilatant behavior was observed, while Newtonian behavior was predominant at lower sizes.

In addition, lower viscosities were measured as the slit size was reduced, due to the minimal hydrodynamic effects caused on the nanoparticles' surface. A reduction of 47.3% in the viscosity of the nanofluid was observed when the slit size changed from 500 to 300 µm at 25 ºC. Furthermore, the viscosity of the nanofluid decreased as much as 60% when the slit size was reduced from 500 to 100 µm.

Moreover, as the temperature was increased, the viscosity of the nanofluid tended to decrease. At high shear rates and keeping the slit size constant, there was a decrease in the viscosity of ~25.2% when the temperature varied from 15 to 25 ºC, while a variation of ~4.6% was observed from 25 to 35 ºC. The viscosity decreased as the slit size was decreased, reaching a reduction of 47.3% when the size changed from 500 to 300 µm at 25 ºC. Viscosities in the range (0.585 – 0.974) mPa·s, (0.716 – 1.124) mPa·s and (1.008 – 1.417) mPa·s were measured at 100, 300 and 500 µm, respectively. Nevertheless, the pH did not influence significantly the rheological behavior of the silver nanofluid flowing in microchannel.

ACKNOWLEDGEMENTS

Authors acknowledge CNPq (Brazilian Council of Scientific and Technological Development) for the financial support. Authors also acknowledge TNS Nanotechnology for kindly supplying the aqueous silver nanosuspension.

REFERENCES

Aberoumand, S., Jafarimoghaddam, A., Moravej, M., Aberoumand, H. and Javaherdeh, K., Experimental study on the rheological behavior of silver-heat transfer oil nanofluid and suggesting two empirical based correlations for thermal conductivity and viscosity of oil based nanofluids, Appl. Therm. Eng., 101, 362-372 (2016). https://doi.org/10.1016/j.applthermaleng.2016.01.148

Afrand, M., Toghraie, D. and Ruhani, B., Effects of temperature and nanoparticles concentration on rheological behavior of Fe_3O_4-Ag/EG hybrid nanofluid: an experimental study, Exp. Therm. Fluid Sci., 77, 38-44 (2016). https://doi.org/10.1016/j.expthermflusci.2016.04.007

Chandrasekar, M., Suresh, S. and Bose, A.C., Experimental investigations and theoretical determination of thermal conductivity and viscosity of Al_2O_3/water nanofluid, Exp. Therm. Fluid Sci., 34, 210-216 (2010). https://doi.org/10.1016/j.expthermflusci.2009.10.022

Chen, C.N., Huang, C.T., Tseng, W.J. and Wei, M.H., Dispersion and rheology of surfactant-mediated silver nanoparticle suspensions, Appl. Surf. Sci., 257, 650-655 (2010). https://doi.org/10.1016/j.apsusc.2010.07.057

Chen, H., Ding, Y. and Tan, C., Rheological behaviour of nanofluids, New J. Phys., 367, 1-24 (2007). https://doi.org/10.1088/1367-2630/9/10/367

Chen, L., Xie, H., Li, Y. and Yu, W., Nanofluids containing carbon nanotubes treated by mechanochemical reaction, Thermochim. Acta, 477, 21-24 (2008). https://doi.org/10.1016/j.tca.2008.08.001

Delay, M., Dolt, T., Woellhaf, A., Sembritzki, R. and Frimmel, F.H., Interactions and stability of silver nanoparticles in the aqueous phase: Influence of natural organic matter (NOM) and ionic strength, J. Chromatogr. A, 1218, 4206-4212 (2011). https://doi.org/10.1016/j.chroma.2011.02.074

Du, L., Wang, Y., Zhang, W., Shen, C. and Luo, G., Preparation of nonaqueous silver nanosuspensions by in situ dispersion of the surface-modified nanoparticles, Colloid Surface A, 501, 114-121 (2016). https://doi.org/10.1016/j.colsurfa.2016.04.044

Elzey, S., and Grassian, V.H., Agglomeration, isolation and dissolution of commercially manufactured silver nanoparticles in aqueous environments, J. Nanopart. Res., 12, 1945-1958 (2010). https://doi.org/10.1007/s11051-009-9783-y

Ewoldt, R.H., Johnston, M.T., and Caretta, L.M. Complex Fluids in Biological Systems, Chap. 6: Experimental challenges of shear rheology: how to avoid bad data. Springer, New York (2015). https://doi.org/10.1007/978-1-4939-2065-5_6

Fischer, A., Application Note: Improved torque sensitivity and normal force resolution for routine measurements, Thermo Fisher Scientific (2007).

Fullman, R.L., Measurement of particle size in opaque bodies, Journal of Metals, 447-452 (1953). https://doi.org/10.1007/BF03398971

Georgieva, K., Dijkstra, D.J., Fricke, H. and Willenbacher, N., Clogging of microchannels by nano-particles due to hetero-coagulation in elongational flow, J. Colloid Interf. Sci., 352, 265-277 (2010). https://doi.org/10.1016/j.jcis.2010.08.065

Ghadimi, A., Saidur, R. and Metselaar, H.S.C., A review of nanofluid stability properties and characterization in stationary conditions, Int. J. Heat Mass Tran., 54, 4051-4068 (2011). https://doi.org/10.1016/j.ijheatmasstransfer.2011.04.014

Haghighi, E.B., Utomo, A.T., Ghanbarpour, M., Zavareh, A.I.T., Nowak, E., Khodabandeh, R., Pacek, A.W. and Palm, B., Combined effect of physical properties and convective heat transfer coefficient of nanofluids on their cooling efficiency, Int. Commun. Heat Mass, 68, 32-42 (2015). https://doi.org/10.1016/j.icheatmasstransfer.2015.08.011

Hedayati, F. and Domairry, G., Nanoparticle migration effects on fully developed forced convection of TiO_2-water nanofluid in a parallel plate microchannel, Particuology, 24, 96-107 (2015). https://doi.org/10.1016/j.partic.2014.11.012

Ho, C.J., Wei, L.C. and Li, Z.W., An experimental investigation of forced convective cooling performance of a microchannel heat sink with Al_2O_3/water nanofluid, Appl. Therm. Eng., 30, 96-103 (2010). https://doi.org/10.1016/j.applthermaleng.2009.07.003

Hojjat, M., Etemad, S.Gh., Bagheri, R. and Thibault, J., Thermal conductivity of non-Newtonian nanofluids: experimental data and modeling using neural network, Int. J. Heat Mass, 54, 1017-1023 (2011). https://doi.org/10.1016/j.ijheatmasstransfer.2010.11.039

Keramati, H., Saidi, M.H. and Zabetian, M., Stabilization of the suspension of zirconia microparticle using the nanoparticle halos mechanism: zeta potential effect, Journal of Dispersion Science and Technology, 37, 6-13 (2015). https://doi.org/10.1080/01932691.2015.1015077

Kole, M. and Dey, T.K., Viscosity of alumina nanoparticles dispersed in car engine coolant, Exp. Therm. Fluid Sci., 34, 677-683 (2010). https://doi.org/10.1016/j.expthermflusci.2009.12.009

Kumpulainen, T., Pekkanen, J., Valkama, J., Laakso, J., Tuokko, R. and Mäntysalo, M., Low temperature nanoparticle sintering with continuous wave and pulse lasers, Opt. Laser Technol., 43, 570-576 (2011). https://doi.org/10.1016/j.optlastec.2010.08.002

Leo, B.F., Chen, S., Kyo, Y., Herpoldt, K.L., Terrill, N.J., Dunlop, I.E., McPhail, D.S., Shaffer, M.S., Schwander, S., Gow, A., Zhang, J., Chung, K.F., Tetley, T.D., Porter, A.E., and Ryan, M.P., The stability of silver nanoparticles in a model of pulmonary surfactant, Environ. Sci. Technol., 47, 11232-11240 (2013). https://doi.org/10.1021/es403377p

Lin, S., Cheng, Y., Liu, J. and Wiesner, M.R., Polymer coatings on silver nanoparticles hinder autoaggregation but enhance attachment to uncoated surfaces, Langmuir, 28, 4178-4186 (2012). https://doi.org/10.1021/la202884f

Lotfizadeh, S., Aljama, H., Reilly, D. and Matsoukas, T., Formation of reversible clusters with controlled degree of aggregation, Langmuir, 32, 4862-4867 (2016). https://doi.org/10.1021/acs.langmuir.6b00746

Mahbubul, I.M., Saidur, R. and Amalina, M.A., Latest developments on the viscosity of nanofluids, Int. J. Heat Mass, 55, 874-885 (2012). https://doi.org/10.1016/j.ijheatmasstransfer.2011.10.021

Mahbubul, I.M., Saidur, R. and Amalina, M.A., Influence of particle concentration and temperature on thermal conductivity and viscosity of Al_2O_3/R141b nanorefrigerant, Int. Commun. Heat Mass, 43, 100-104 (2013). https://doi.org/10.1016/j.icheatmasstransfer.2013.02.004

Mohammed, H.A., Bhaskaran, G., Shuaib, N.H. and Saidur, R., Heat transfer and fluid flow characteristics in microchannels heat exchanger using nanofluids: a review, Renew. Sust. Energ. Rev., 15, 1502-1512 (2011). https://doi.org/10.1016/j.rser.2010.11.031

Mostafizur, R.M., Abdul Aziz, A.R., Saidur, R., Bhuiyan, M.H.U. and Mahbubul, I.M., Effect of temperature and volume fraction on rheology of methanol based nanofluids, Int. J. Heat Mass, 77, 765-769 (2014). https://doi.org/10.1016/j.ijheatmasstransfer.2014.05.055

Namburu, P.K., Kulkarni, D.P., Misra, D. and Das, D.K., Viscosity of copper oxide nanoparticles dispersed in ethylene glycol and water mixture, Exp. Therm. Fluid Sci., 32, 397-402 (2007). https://doi.org/10.1016/j.expthermflusci.2007.05.001

Oliveira, G.A., Wen, D.S. and Filho, E.P.B., Synthesis and characterization of silver/water nanofluids, High Temp.–High Press., 43, 69-83 (2014).

Parametthanuwat, T., Bhuwakietkumjohn, N., Rittidech, S. and Ding, Y., Experimental investigation on thermal properties of silver nanofluids, Int. J. Heat Fluid Fl., 56, 80-90 (2015). https://doi.org/10.1016/j.ijheatfluidflow.2015.07.005

Parks, G.A., The isoelectric points of solid oxides, solid hydroxides, and aqueous hydroxo complex systems, Chem. Rev., 65, 177-198 (1965). https://doi.org/10.1021/cr60234a002

Paul, G., Sarkar, S., Pal, T., Das, P.K. and Manna, I., Concentration and size dependence of nano-silver dispersed water based nanofluids, J. Colloid Interf. Sci., 371, 20-27 (2012). https://doi.org/10.1016/j.jcis.2011.11.057

Rao, K.D., Vasukiran, M., Gollakota, A.R.K., and Kishore, N., Buoyancy driven bubble rise and deformation in milli/micro channels filled with shear-thinning nanofluids, Colloid. Surface A, 467, 66-77 (2015). https://doi.org/10.1016/j.colsurfa.2014.11.030

Sadowski, Z., Maliszewska, I.H., Grochowalska, B., Polowczyk, I., and Kozlecki, T., Synthesis of silver nanoparticles using microorganisms, Mater. Sci.-Poland, 26, 419-424 (2008).

Sharma, A.K., Tiwari, A.K. and Dixit, A.R., Rheological behavior of nanofluids: a review, Renew. Sust. Energ. Rev., 53, 779-791 (2016). https://doi.org/10.1016/j.rser.2015.09.033

Shi, Y.Y., Sun, B., Zhou, Z., Wu, Y.T. and Zhu, M.F., Size-controlled and large-scale synthesis of organic-soluble Ag nanocrystals in water and their formation mechanism, Prog. Nat. Sci-Mater, 21, 447-454 (2011). https://doi.org/10.1016/S1002-0071(12)60081-1

Shoghl, S.N., Jamali, J. and Moraveji, M.K., Electrical conductivity, viscosity, and density of different nanofluids: an experimental study, Exp. Therm. Fluid Sci., 74, 339-346 (2016). https://doi.org/10.1016/j.expthermflusci.2016.01.004

Singh, A. and Raykar, V.S., Microwave synthesis of silver nanofluids with polyvinylpyrrolidone (PV) and their transport properties, Colloid Polym. Sci., 286, 1667-1673 (2008). https://doi.org/10.1007/s00396-008-1932-9

Singh, P.K., Harikrishna, P.V., Sundararajan, T. and Das, S.K., Experimental and numerical investigation into the hydrodynamics of nanofluids in microchannels, Exp. Therm. Fluid Sci., 42, 174-186 (2012). https://doi.org/10.1016/j.expthermflusci.2012.05.004

Sohrabi, S., Yunus, D.E., Xu, J., Yang, J. and Liu, Y., Characterization of nanoparticle binding dynamics in microcirculation using an adhesion probability function, Microvasc. Res., 108, 41-47 (2016). https://doi.org/10.1016/j.mvr.2016.07.005

Sridhara, V. and Satapathy, L.N., Al_2O_3-based nanofluids: a review, Nanoscale Res. Lett., 6, 456-472 (2011). https://doi.org/10.1186/1556-276X-6-456

Sundar, L. and Sharma, K.V., Heat transfer enhancements of low volume concentration Al_2O_3 nanofluid and with longitudinal strip inserts in a circular tube, Int. J. Heat Mass, 53, 4280-4286 (2010). https://doi.org/10.1016/j.ijheatmasstransfer.2010.05.056

Tamjid, E. and Guenther, B.H., Rheology and colloidal structure of silver nanoparticles dispersed in diethylene glycol, Powder Technol., 197, 49-53 (2010). https://doi.org/10.1016/j.powtec.2009.08.022

Yao, D. and Kim, B., Simulation of the filling process in micro channels for polymeric materials, J. Micromec. Microeng., 12, 604-610 (2002). https://doi.org/10.1088/0960-1317/12/5/314